

CHEMISTRY

A European Journal

A Journal of



Accepted Article

Title: Twisted Polycyclic Arenes from Diphenyltetranaphthylbenzenes by Controlling the Scholl Reaction with Substituents

Authors: Yong Yang, Luyan Yuan, Bowen Shan, Zhifeng Liu, and Qian Miao

This manuscript has been accepted after peer review and appears as an Accepted Article online prior to editing, proofing, and formal publication of the final Version of Record (VoR). This work is currently citable by using the Digital Object Identifier (DOI) given below. The VoR will be published online in Early View as soon as possible and may be different to this Accepted Article as a result of editing. Readers should obtain the VoR from the journal website shown below when it is published to ensure accuracy of information. The authors are responsible for the content of this Accepted Article.

To be cited as: *Chem. Eur. J.* 10.1002/chem.201604649

Link to VoR: <http://dx.doi.org/10.1002/chem.201604649>

Supported by
ACES

WILEY-VCH

Twisted Polycyclic Arenes from Diphenyltetranaphthylbenzenes by Controlling the Scholl Reaction with Substituents

Yong Yang, Luyan Yuan, Bowen Shan, Zhifeng Liu, and Qian Miao*

Abstract: We herein report two novel types of twisted polycyclic arenes (**2a,b** and **3a,b**) with constitutionally isomeric π -backbones, which are synthesized by controlling the Scholl reaction of 1,2,4,5-tetra(naphth-2-yl)-3,6-diphenylbenzene (**1**) with properly positioned electron-donating substituents. With a polycyclic backbone containing two [5]helicene and four [4]helicene moieties, **2a,b** are new members of multiple helicenes with interesting stereochemistry. The as-synthesized **2a,b** are the twisted isomer, and the thermal isomerization of twisted-**2b** results in *anti*-**2b**, a more stable stereoisomer. Both twisted and *anti*-**2b** have been fully characterized, and the thermal isomerization of twisted-**2b** has been studied with ^1H NMR spectroscopy and DFT calculation. **3a,b** are new members of twistacenes, whose benzannulated pentacene backbone exhibit an end-to-end twist as found from the crystal structure. Twisted and *anti*-**2b** are also found to function as p-type semiconductors in solution-processed thin film transistors, while the thin films of **3b** appear insulating presumably due to lack of π - π interactions.

Introduction

The Scholl reaction is a powerful method for synthesis of polycyclic arenes by intramolecular oxidative cyclodehydrogenation forming multiple carbon-carbon bonds in a single step.^[1] This method was pioneered by Scholl in 1910,^[2, 3] and developed by Müllen for preparing functionalized hexa-*peri*-hexabenzocoronenes (HBCs) from hexaphenylbenzene precursors.^[4, 5] A variety of polyphenylenes have been used as substrates in the Scholl reactions leading to nanographenes with different size.^[6] More recently, the Scholl reaction has been successfully utilized for synthesis of non-planar polycyclic arenes in connection with the interests to explore the possibilities of π systems to approach novel carbon nanomaterials.^[7, 8, 9] To our surprise, the Scholl reaction of 1,2,4,5-tetra(naphth-2-yl)-3,6-diphenylbenzene (**1** in Figure 1), an undocumented analogue of hexaphenylbenzene^[10] with a closely related structure, was not reported. Here we report the Scholl reaction of substituted tetranaphthylidiphenylbenzenes, which leads to two novel types of twisted polycyclic arenes (**2a,b** and **3a,b** in Figure 1) depending on the substituting groups.

The parent hydrocarbon molecules of **2a,b** and **3a,b** are **2c** and **3c**, respectively, which are a pair of constitutional isomers with the same molecular formula of $\text{C}_{58}\text{H}_{30}$. They are both forced out of planarity by steric strains from atom crowding, but apparently differ in the way of twisting. **2c** is a multiple helicene

containing two [5]helicene and four [4]helicene moieties, which present local helical structures as a consequence of the repulsive steric interactions between terminal benzene rings in the *ortho*-fused backbone. The combination of local helicity in a multiple helicene^[11] provides molecular dynamics and defines three-dimensional molecular shape as well as molecular packing in crystalline state.^[12] Here we define the multiple helicity of **2a-c** as (*H1*, *H2*)-(*h3*, *h4*, *h5*, *h6*), where the helicity notions in the first pair of parentheses refer to the [5]helicene moieties and those in the second pair of parentheses refer to the [4]helicene moieties as depicted in Figure 1. Having a benzannulated pentacene backbone substituted with two phenyl groups, **3c** exhibits an end-to-end twist as found from the energy-minimized model (Figure S3 in the Supporting Information). Therefore it can be regarded as a new member of twistacenes^[13], which were reported by Pascal,^[14, 15] Wudl^[16] and Zhang.^[17] Detailed below are the synthesis and structures of **2a,b** and **3a,b**, stereoisomers and isomerization of **2a/b**, and a brief investigation of semiconductor properties of **2b**.

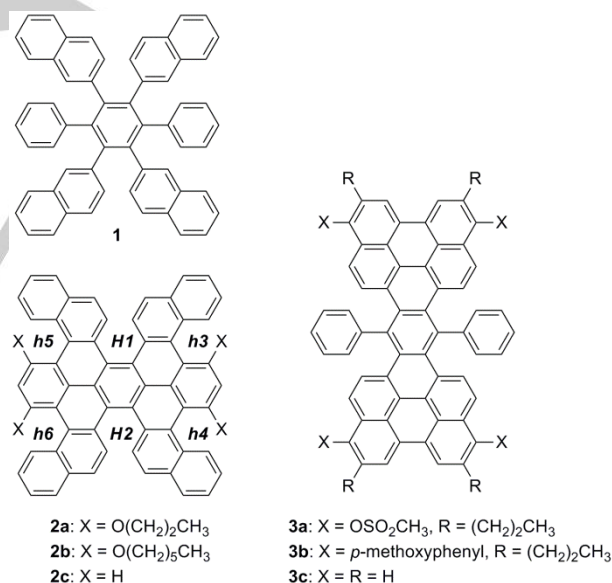


Figure 1. Molecular structures of tetranaphthylidiphenylbenzene **1** and twisted polycyclic arenes **2a,b** and **3a,b**.

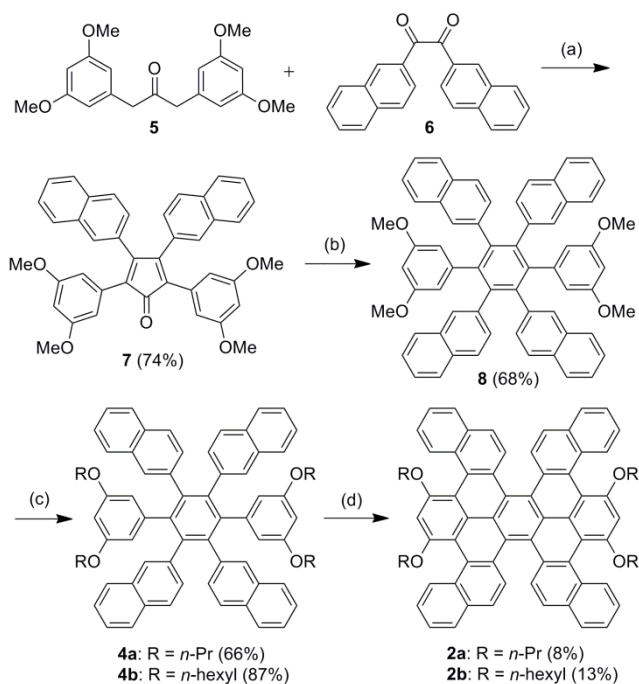
Results and Discussion

Synthesis

Shown in Scheme 1 is the synthesis of **2a,b** by the Scholl reaction of alkoxyated diphenyltetra(naphth-2-yl)benzenes **4a,b**, which were prepared by modifying the earlier reported synthesis of alkoxyated hexaphenylbenzenes.^[8] Two of the naphth-2-yl groups in **4a,b** were introduced by double aldol condensation of ketone **5**^[8] and di(naphth-2-yl)ethanedione (**6**), and the other

Y. Yang, L. Yuan, B. Shan, Prof. Dr. Z. Liu, Prof. Dr. Q. Miao
 Department of Chemistry
 The Chinese University of Hong Kong
 Shatin, New Territories, Hong Kong, China
 E-mail: miaoqian@cuhk.edu.hk

Supporting information for this article is given via a link at the end of the document.

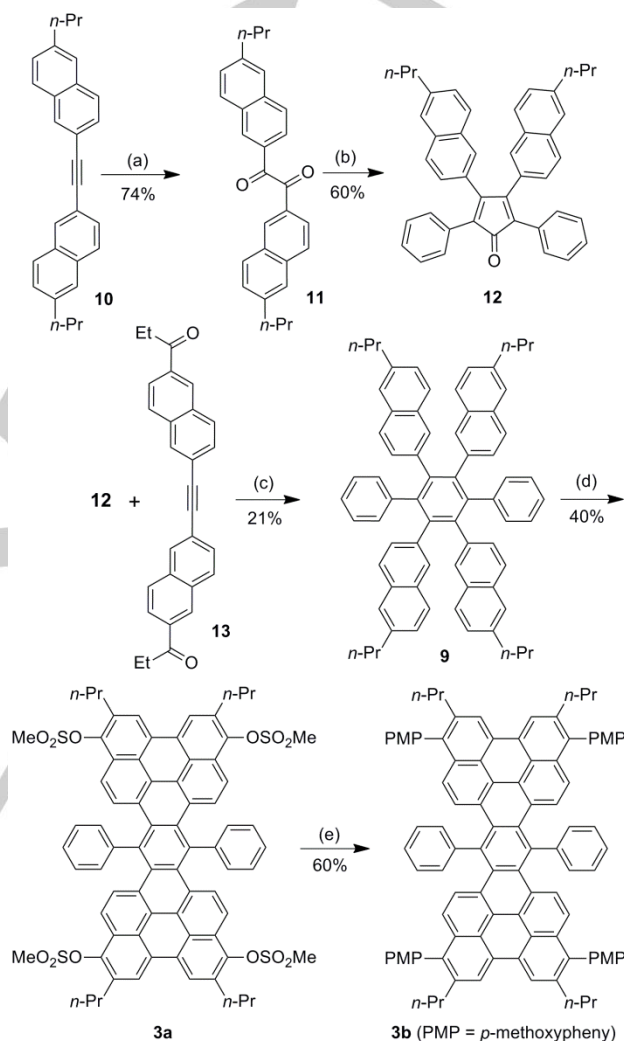


Scheme 1. Synthesis of **2a,b**: (a) KOH, C₂H₅OH; (b) di(2-naphthyl)acetylene, diphenyl ether, reflux; (c) (i) BBr₃, CH₂Cl₂; (ii) K₂CO₃, C₃H₇Br for **2a** or C₆H₁₃Br for **2b**, DMF; (d) DDQ, CH₃SO₃H, CH₂Cl₂.

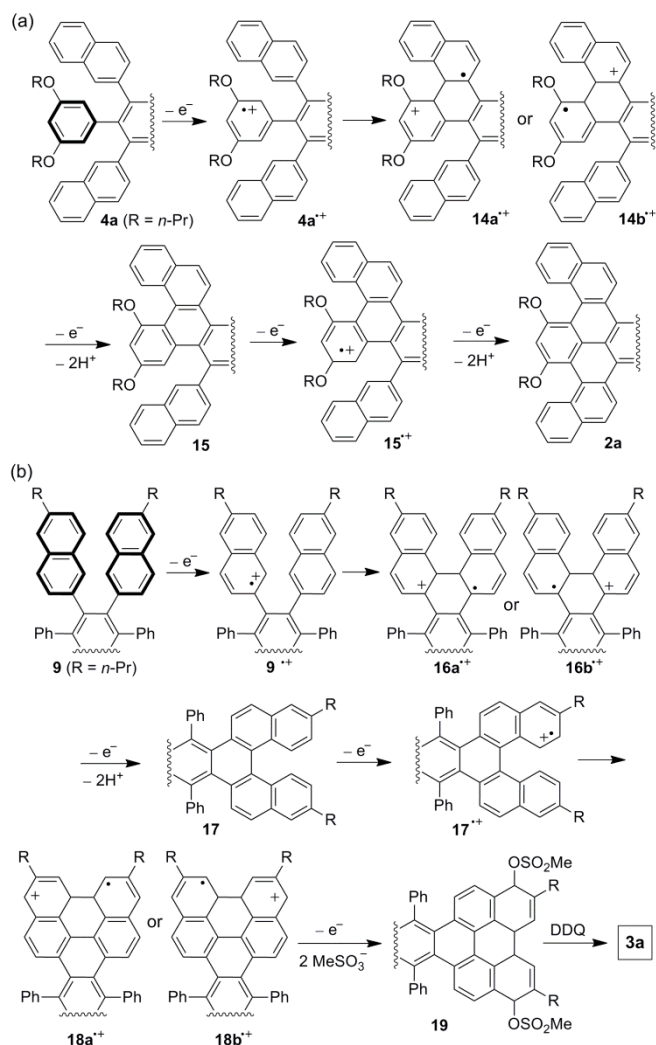
two naphth-2-yl groups were introduced by the Diels–Alder cycloaddition of **7** and di(naphth-2-yl)acetylene. In order to increase solubility of the final product, the methyl groups in **8** were replaced by propyl and hexyl groups before oxidative cyclodehydrogenation. The Scholl reaction of **4a,b** in acidic condition with DDQ as oxidant^[18] resulted in **2a,b** in low yields presumably because each naphthyl group can react either at the more reactive α position or the less reactive β position.^[19] In comparison to this condition, treatment of **4a,b** with FeCl₃, a conventional oxidant for the Scholl reaction, led to a complicated mixture, from which **2a,b** were not isolated. The multiple helicene structure of **2a,b** was finally confirmed with the single crystal structures as detailed in the latter part of this article.

Shown in Scheme 2 is the synthesis of **3a** and **3b** from propyl-substituted di(naphth-2-yl)acetylene **10**, which was prepared by modifying the reported synthesis of hexyl-substituted di(naphth-2-yl)acetylene.^[20] Palladium-catalyzed oxidation of **10** led to dione **11**, which, similar to **6**, underwent double aldol condensation yielding **12**. The Diels–Alder cycloaddition of **12** with **10** resulted in **9** in a yield as low as 5%, while the Diels–Alder cycloaddition of **12** with a more electron-deficient dienophile **13** followed by reduction of the two carbonyl groups led to **9** in a higher yield of 21%. Unlike **4a** with two propoxy groups attached to each phenyl group, **9** has two unsubstituted phenyl groups and has its naphth-2-yl groups each equipped with a propyl substituent as the solubilizing group. Treatment of **9** with 8.5 equivalents of DDQ at the presence of excessive methanesulfonic acid resulted in **3a** in a yield of 40%, but did not lead to isolation of a multiple helicene with the same

polycyclic backbone as **2a**. In comparison to this condition, treatment of **9** with FeCl₃ did not lead to cyclized products that could be isolated and characterized. Further reaction of **3a** with 4-methoxyphenylboronic acid in a nickel-catalyzed cross coupling reaction yielded **3b**, whose twistacene backbone was finally confirmed with the single crystal structure as detailed in the latter part of this article.



Scheme 2. Synthesis of **3a,b**: (a) Pd(OAc)₂, CuBr₂, DMSO; (b) 1,3-diphenylacetone, KOH, EtOH; (c) (i) diphenyl ether, reflux, (ii) triethylsilane, CF₃COOH; (d) DDQ, CH₃SO₃H, CH₂Cl₂; (e) 4-methoxyphenylboronic acid, Ni(COD)₂, tricyclohexylphosphine, K₃PO₄, toluene.



Scheme 3. Proposed mechanism for the formation of (a) **2a** and (b) **3a**. (For clarification, the radical and cation are shown as localized rather than delocalized and their resonance structures are not shown).

The different outcomes of the above two Scholl reactions can be understood by considering the most reactive site of the substrate in the cation-radical (electron transfer) mechanism.^[21] With two electron-donating substituents, the alkoxyated phenyl ring (shown with bold lines in Scheme 3a) is the most electron-rich part in **4a**, in agreement with the calculated highest occupied molecular orbital (HOMO) of **4a**, which is localized on the alkoxyated phenyl rings as shown in Figure S4 in the Supporting Information. In contrast, the alkylated naphthalene rings as shown with bold lines in Scheme 3b are the most electron-rich part in **9**, in agreement with the calculated HOMO of **9**, which is localized on the naphthalene rings as shown in Figure S4 in the Supporting Information. Therefore, upon oxidation by DDQ/H⁺, the alkoxyated phenyl ring in **4a** loses one electron yielding a cation-radical (**4a⁺**), which couples with a neighboring naphthyl group resulting in another cation radical (**14a⁺** or **14b⁺**) with formation of a C-C bond. Further

oxidation with one more electron transfer and elimination of two protons leads to the intermediate **15** with aromatization. Repeated reactions on the alkoxyated benzene rings finally lead to **2a,b** with incomplete cyclodehydrogenation similar to the earlier reported synthesis of alkoxyated hexabenzoperylene.^[8] In contrast, the naphthalene ring in **9** is the favored reaction site upon oxidation by DDQ/H⁺ resulting in the corresponding radical cation (**9⁺**), where the positively charged naphthyl group is adjacent to both naphthyl and phenyl groups. Because a naphthalene ring is more reactive than a benzene ring forming a cation or radical that retains aromaticity, the coupling reaction occurs between the two naphthyl groups putting a radical or cation on the second naphthyl group. Further oxidation of the resulting cation radical (**16a⁺** or **16b⁺**) and elimination of two protons lead to the aromatized intermediate **17**, which loses one electron still in the naphthalene moiety leading to the corresponding radical cation (**17⁺**). The intramolecular coupling reaction of **17⁺** leads to another cation radical (**18a⁺** or **18b⁺**), which is further oxidized and quenched by methanesulfonate resulting in **19**. Aromatization of **19** by dehydrogenation with DDQ leads to **3a**. With the above discussion, we conclude that the reactivity of **1** in the Scholl reaction can be controlled by suitably placed strongly activating groups.^[22]

Stereoisomers and isomerization of **2a,b**

The conjugated backbone of **2a,b** is a multiple helicene (**2c**) containing two [5]helicene and four [4]helicene moieties. With the six-fold helicity, **2a,b** each have 24 stereoisomers including 10 pairs of enantiomers and 4 meso isomers as shown in Figure S1 in the Supporting Information. Because [4]helicene has a small racemization barrier of 14.6 to 31.8 kJ/mol as calculated with different methods,^[23] the stereoisomers due to different helicity of the [4]helicene moieties can in principle interconvert rapidly with each other in solution at room temperature. In contrast, the different helicity of the [5]helicene moieties in **2a,b** is expected to result in stable isomers that can be isolated at room temperature because [5]helicene has a much higher racemization barrier (calculated with different methods as 95.0 to 133.9 kJ/mol and experimentally determined as 95.0 kJ/mol).^[23, 24] To determine the stereochemistry of **2a,b**, red crystals of **2a** grown from solution in 1,2-dichloroethane-ethyl acetate were subjected to X-ray diffraction. The crystal structure of **2a**^[25] reveals a chiral twisted backbone as defined by the two [5]helicene moieties, and a unit cell contains two pairs of enantiomers of twisted-**2a**. Figure 2a shows one enantiomer having the (*P, P*)-(*M, P, P, M*) helicity together with the dihedral angle between two terminal benzene rings for each helicene moiety.²⁶ Figure 2b shows the unit cell of twisted-**2a** with the (*P, P*)-(*M, P, P, M*) stereoisomer colored in yellow and its enantiomer colored in cyan. It is found that two neighboring enantiomers of twisted-**2a** stack with each other with overlap of about four benzene rings and intermolecular C-to-C contacts of about 3.5 Å. Here the distance between π -planes for this π - π interaction (shown with the red double-head arrows) cannot be measured because the overlapped benzene rings in the non-planar backbone are not parallel to each other. In contrast, the intermolecular π - π interactions between adjacent molecules of

the same handedness are negligible. Because **2a** and **2b** exhibit almost identical ^1H NMR spectra in the aromatic range, it is concluded that the as-synthesized **2b** is also the twisted stereoisomer (twisted-**2b**).

In order to find other stereoisomers of **2a,b** with different helicity of the [5]helicene moieties, the more soluble derivative twisted-**2b** was subjected to heating. Refluxing a solution of twisted-**2b** in toluene under an atmosphere of nitrogen for two hours led to a new orange compound with almost complete conversion of twisted-**2b**. This orange compound was purified by chromatography on silica gel, and was determined as an isomer of twisted-**2b** based on the ^1H NMR and mass spectra. Single crystals of this orange compound were grown from CH_2Cl_2 -ethyl acetate and were subjected to X-ray diffraction. The crystal structure reveals an achiral stereoisomer of **2b** with *anti*-folded conformation.^[24] Figure 3a shows the backbone of *anti*-**2b**, which has the (*M, P*)-(*P, M, P, M*) helicity and is more curved than twisted-**2a** in the [5]helicene moieties with a larger dihedral angle. With slightly different dihedral angles for the [4]helicene moieties, *anti*-**2b** is C_i symmetric rather than C_{2h} symmetric in the crystal. As shown in Figure 3b, molecules of *anti*-**2b** are packed in the crystal exhibiting face-to-face π -stacking between the terminal naphthalene rings of the adjacent molecules with relatively large π -to- π distance of about 3.6 Å.

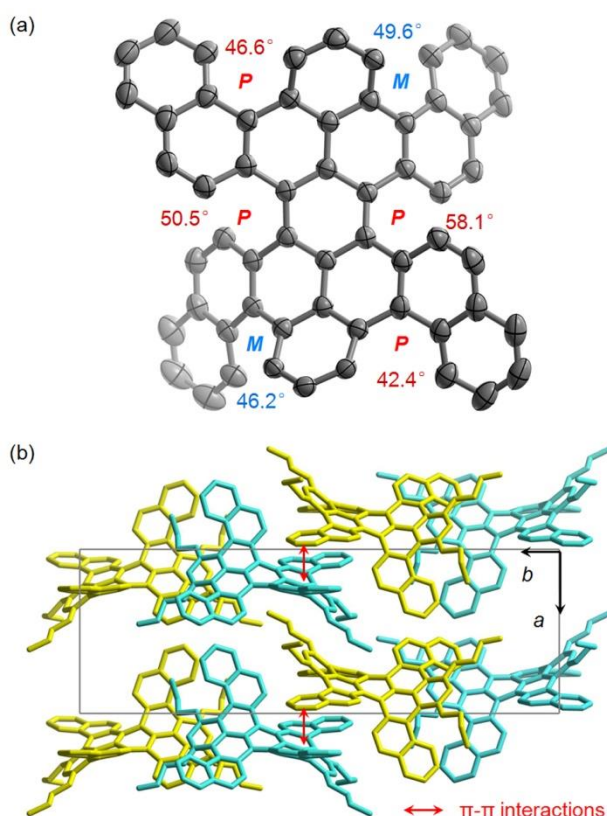


Figure 2. Crystal structure of **2a**: (a) the (*P, P*)-(*M, P, P, M*) enantiomer of **2a** with the propoxyl groups and hydrogen atoms removed and carbon atom positions shown as 50% probability ellipsoids; (b) a unit cell of **2a** with hydrogen atoms removed for clarity as viewed along the *c* axis.

In agreement with its red color, twisted-**2b** exhibits a red-shifted absorption spectrum relative to that of *anti*-**2b** as shown in Figure 4. This may be attributed to severer distortion of its central benzene ring, which leads to redistribution of electrons in HOMO and LUMO. The fluorescence spectra of twisted-**2b** and *anti*-**2b** exhibit Stokes shifts of 43 nm and 57 nm, respectively. These relatively large Stokes shifts are in agreement with the fact that the twisted and *anti*-folded backbones of **2b** are flexible in solution by flipping at the [4]helicene moieties thus consuming the energy of the excited state. The twisted and *anti*-folded isomers of **2b** differ not only in photophysical properties but also in electrochemistry. The cyclic voltammogram of two isomers of **2b** in CH_2Cl_2 (Figure S6 in the Supporting Information) exhibit two reversible oxidation waves, which have the half-wave potential at 0.12 and 0.31 V vs ferrocenium/ferrocene for twisted-**2b** and at 0.38 and 0.53 V vs ferrocenium/ferrocene for *anti*-**2b**, respectively. From the first oxidation potential, the HOMO energy level is estimated as -5.22 eV for twisted-**2b** and -5.48 eV for *anti*-**2b**, respectively.^[27]

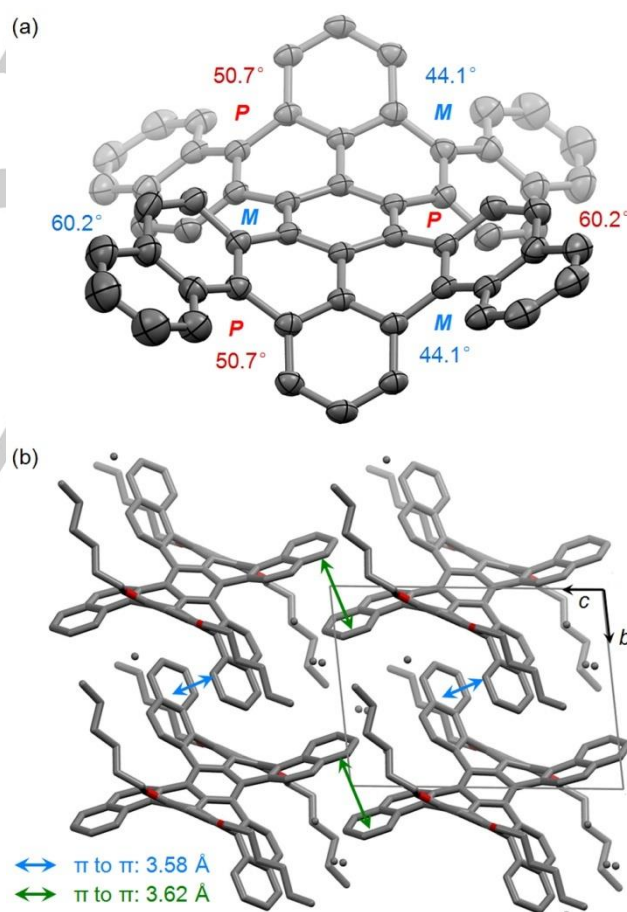


Figure 3. Crystal structure of *anti*-**2b**: (a) *anti*-**2b** with the hexoxyl groups and hydrogen atoms removed and carbon atom positions shown as 50% probability ellipsoids; (b) molecular packing of *anti*-**2b** with hydrogen atoms removed for clarity. (Disordered carbon atoms in the hexyl groups are shown as dots.)

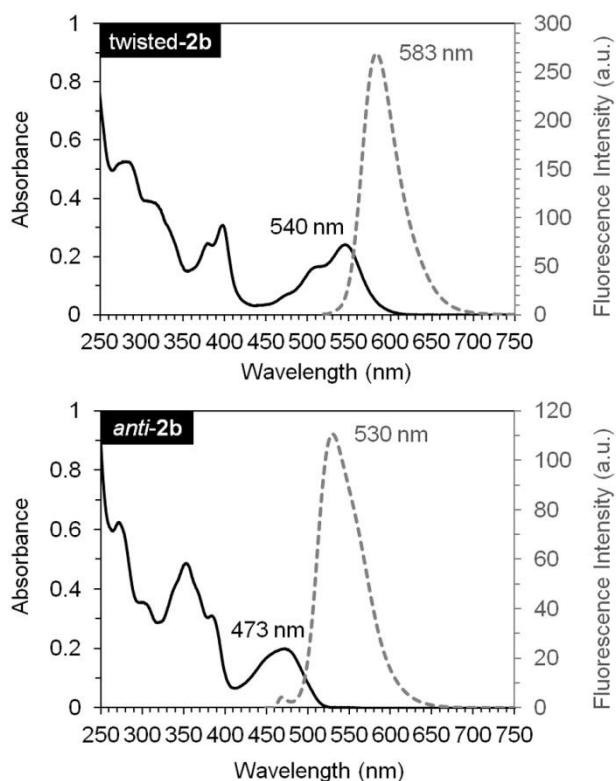


Figure 4. UV-vis absorption and fluorescence (excited at 530 nm and 465 nm, respectively) spectra of twisted-**2b** (top) and *anti*-**2b** (bottom) in CH_2Cl_2 (5×10^{-6} mol/L).

The thermal isomerization of twisted-**2a,b** was studied both computationally and experimentally. In the computational study, a simplified model molecule, **2d**, with methyl groups replacing the longer alkyl groups in **2a,b** as shown in Figure 5, was optimized at the B3LYP/6-31G* level of Density Functional Theory (DFT). It is found that *anti*-**2d** with the (*M, P*)-(*P, M, P, M*) helicity is more stable than twisted-**2d** with the (*P, P*)-(*P, M, M, P*) helicity by 8.0 kJ/mol. Because isomerization of twisted-**2d** to *anti*-**2d** involves inversion of helicity in one [5]helicene moiety (*H1*) and in two [4]helicene moieties (*h5* and *h6*), there are six possible paths for this isomerization based on the sequence of helicity inversion in the three helicene moieties, and each isomerization path contains two intermediates and three transition states. The most plausible isomerization path from twisted-**2d** to *anti*-**2d** with the lowest total activation energy of 121.3 kJ/mol is shown in Figure 5, where the helicene moieties inverting in transition states are highlighted in green. The first step of this path inverts the helicity in the [4]helicene moiety *h6* with an activation energy of 66.5 kJ/mol, which is much larger than the racemization barrier of unsubstituted [4]helicene (14.6 to 31.8 kJ/mol as calculated with different methods)^[23] because of the fused benzene rings and the extra methoxy group. The second step inverts the helicity of the [5]helicene moiety *H1* with an activation energy of 112.9 kJ/mol, and the third step inverts the helicity of the [4]helicene moiety *h5* with an activation energy of 17.6 kJ/mol. In agreement with the calculated energy of the two intermediates in this path, the corresponding unstable stereoisomers of **2a,b** with the (*P, P*)-(*P, M, M, M*) and (*M, P*)-(*P, M, M, M*) helicity were not isolated in our experiments. In

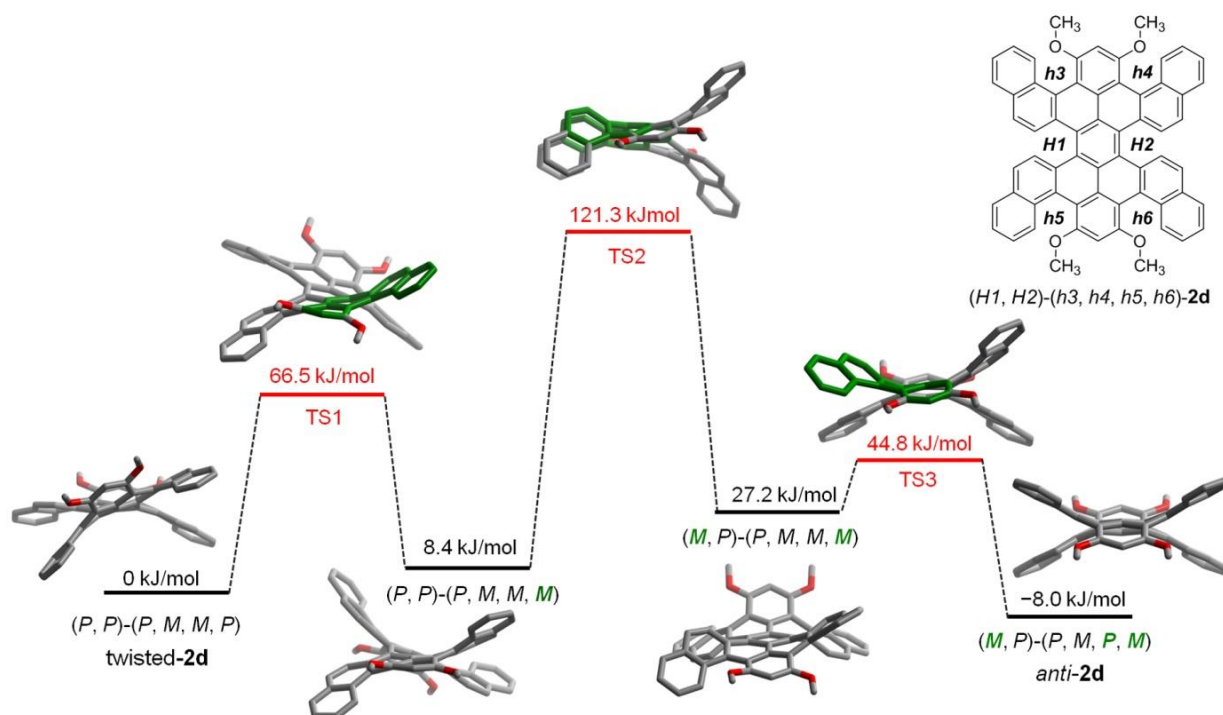


Figure 5. Structures and Gibbs free energies of intermediates and transition states during the most plausible isomerization path from twisted-**2d** to *anti*-**2d** as calculated at the B3LYP/6-31G* level of DFT.

comparison with the isomerization path shown in Figure 5, the other five possible isomerization paths with higher activation energy are shown in Figure S2 in the Supporting Information.

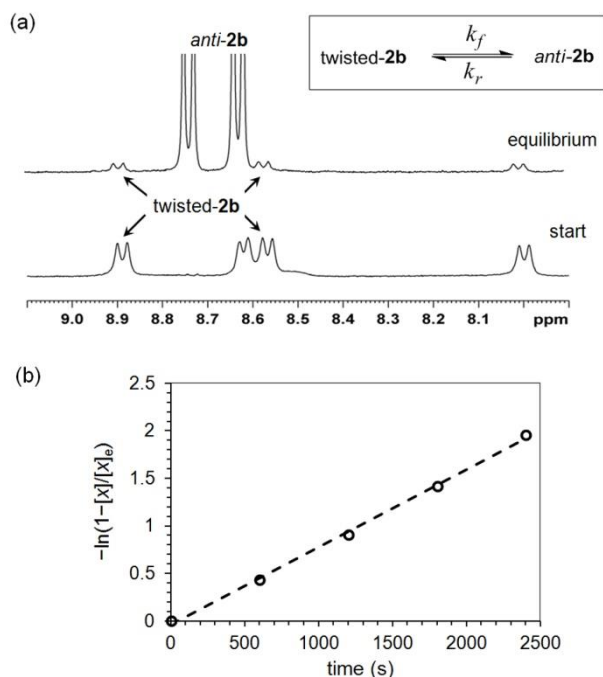


Figure 6. Isomerization of **2b** as monitored by ^1H NMR (400 MHz) spectroscopy: (a) selected ^1H NMR spectra of twisted-**2b** and *anti*-**2b** during the progress of twisted-to-*anti* isomerization in toluene- d_6 at 105 °C; (b) a plot of $-\ln(1 - [x]/[x]_e)$ for twisted-**2b** versus time.

To study the thermodynamics and kinetics of thermal isomerization of **2b** experimentally, a solution of twisted-**2b** in toluene- d_6 was heated at 105 °C in a sealed NMR tube, and the progress of isomerization was monitored with ^1H NMR spectroscopy. As shown in Figure 6a, heating twisted-**2b** led to a new set of peaks that belong to *anti*-**2b**, and the ratio of twisted to *anti*-**2b** was determined from the integrations of the corresponding peaks in the ^1H NMR spectra. The ratio of *anti*-**2b** to twisted-**2b** increased to 11 and remained essentially unchanged after the solution was heated for 60 minutes, indicating that the twisted-to-*anti* isomerization reached the equilibrium with an equilibrium constant of 11, from which the free energy change ΔG for the isomerization at 105 °C is determined as 7.5 kJ/mol in agreement with the calculated value (8.0 kJ/mol). The thermal isomerization of twisted-**2b** is a reversible unimolecular reaction, and its rate constants can be estimated by using the equation $-\ln(1 - [x]/[x]_e) = (k_f + k_r)t$, where $[x]$ is the concentration of twisted-**2b** that has been depleted at a certain time t as calculated from the integrations of the NMR peaks for twisted and *anti*-**2b**, $[x]_e$ is defined as $[x]$ at equilibrium, k_f and k_r are the rate constants for the forward and reverse reactions, respectively.^[28] Plotting $-\ln(1 - [x]/[x]_e)$ versus time leads to a slope of $8.1 \times 10^{-4} \text{ s}^{-1}$ as shown in Figure 6b. From this slope and the reaction equilibrium constant $K = k_f / k_r =$

11, the rate constants k_f and k_r at 105 °C are determined as $7.5 \times 10^{-4} \text{ s}^{-1}$ and $6.8 \times 10^{-5} \text{ s}^{-1}$, respectively. Using the Eyring equation $k = \kappa(k_B T/h) \exp(-\Delta G^\ddagger/RT)$ and assuming a value of unity for the transmission coefficient (κ),^[28] the activation free energy ΔG^\ddagger is calculated as 116 kJ/mol for the twisted-to-*anti* isomerization, which is in agreement with the calculated energy barrier for twisted-**2d** (121.3 kJ/mol).

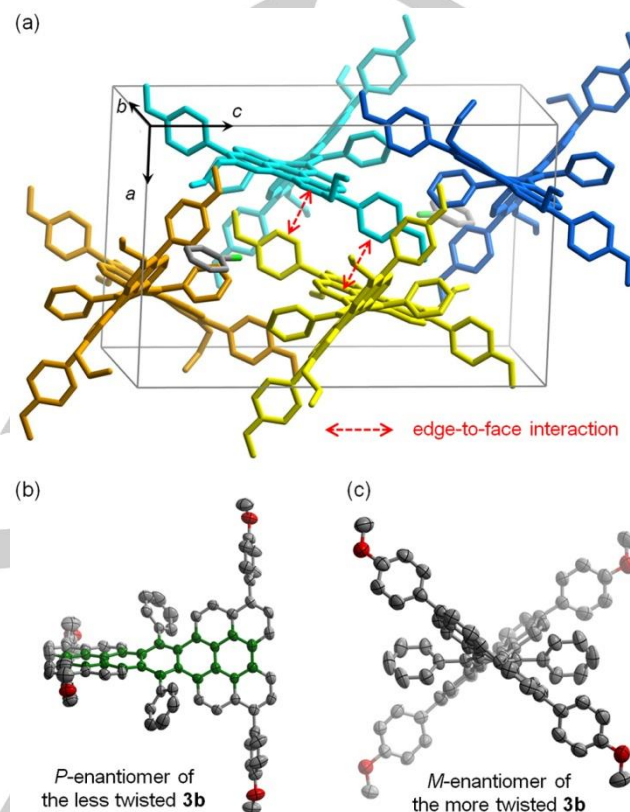


Figure 7. Crystal structure of **3b**·0.5(C₆H₅Cl): (a) a unit cell with the *P*-enantiomers colored in yellow and orange and the *M*-enantiomers colored in cyan and blue; (b) *P*-enantiomer of the less twisted **3b** with the pentacene nucleus highlighted in green and the propyl groups removed for clarity; (c) *M*-enantiomer of the more twisted **3b** with the propyl groups removed for clarity. (Hydrogen atoms are removed for clarity, and carbon atom positions in (b) and (c) are shown as 50% probability ellipsoids.)

Structure and properties of **3b**

Single crystals of **3b** were grown from solution in CH₂Cl₂–chlorobenzene by slow evaporation of solvents, and investigated by X-ray crystallography,^[25] which revealed a chiral backbone of **3b** with an end-to-end twist. As shown Figure 7a, the unit cell of **3b** contains two enantiomeric pairs that are crystallographically independent as well as two molecules of chlorobenzene from the solvent. The crystallographically independent molecules of **3b** differ in the degree of twisting. In Figure 7a, the *P*- and *M*-enantiomers of the less twisted **3b** are shown in yellow and cyan, respectively, while the *P*- and *M*-enantiomers of

the more twisted **3b** are shown in orange and blue, respectively. Figure 7b shows the *P*-enantiomer of the less twisted **3b**, where the end-to-end twist of the pentacene nucleus (shown in green) can be quantified by measuring the torsion angle defined by the four terminal carbon atoms.^[13] The end-to-end twist angle of the pentacene nucleus (shown in green in Figure 7b) in the less twisted and more twisted **3b** is 71.5° and 83.1°, respectively. Therefore **3b** is less twisted than Pascal's hexaphenyltetrabenzo[*a,c,l,n*]pentacene, whose pentacene nucleus exhibits a twist of 144°. ^[15] It is worth noting that the twist of the pentacene nucleus is not evenly distributed in the five rings. In the more twisted **3b**, the central ring is most twisted with an end-to-end twist angle of 25.6°, while the two terminal rings are twisted by only about 10° presumably because they are embedded in the perylene moiety. Figure 7c shows the *M*-enantiomer of the more twisted **3b** as viewed along the long molecular axis. As indicated by the red arrows in Figure 7a, neighbouring enantiomers of **3b** interact with each other in an edge-to-face arrangement with intermolecular carbon–hydrogen contacts of about 3.0 Å.

Compound **3b** is a bright orange solid with strong yellow fluorescence in solution when excited with UV light. As shown in Figure 8, the UV-vis absorption spectrum of **3b** exhibits a band which is characteristic of acenes in the visible light region. The fluorescence spectra of **3b** exhibits a Stokes shift of 15 nm, which is smaller than those of twisted- and *anti*-**2b** suggesting the twistacene backbone of **3b** is more rigid than those of **2b**. The cyclic voltammogram of **3b** in CH₂Cl₂ (Figure S6, in the Supporting Information) exhibits two reversible oxidation waves with the half-wave potential at 0.31 and 0.60 V vs ferrocenium/ferrocene. From the first oxidation potential, the HOMO energy level of **3b** is estimated as -5.41 eV.^[27]

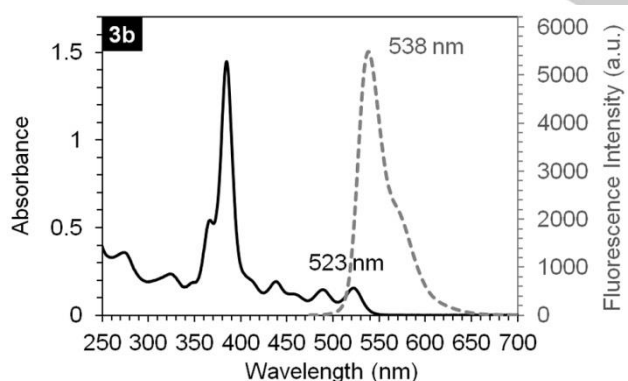


Figure 8. UV-vis absorption and fluorescence (excited at 450 nm) spectra of **3b** in CH₂Cl₂ (5×10^{-6} mol/L).

Semiconductor Properties

As suggested by the relatively high HOMO energy level and the π - π interactions in the crystal structure, twisted-**2b** and *anti*-**2b** can in principle function as p-type semiconductors in the solid

state. To test the semiconductor properties of the two compounds in organic thin film transistors (OTFTs), their thin films were drop-cast onto a silicon substrate, which had successive layers of silica, alumina and 12-cyclohexyldodecylphosphonic acid (CDPA) as a composite dielectric material. Here, CDPA formed a self-assembled monolayer (SAM) on alumina to provide a highly ordered dielectric surface wettable by common organic solvents^[29] and the resulting CDPA-Al₂O₃/SiO₂ had a capacitance per unit area (*C*) of 26 ± 1 nF/cm².^[30, 31] The transistors were completed by depositing a layer of gold onto the organic films through a shadow mask to form top contact source and drain electrodes. As measured in ambient air from these devices, twisted-**2b** and *anti*-**2b** functioned as p-type semiconductors with field effect mobilities of 2×10^{-3} and 1×10^{-3} cm² V⁻¹ s⁻¹, respectively. The typical current-voltage characteristics of these devices are shown in the Supporting Information. The low field effect mobilities of twisted and *anti*-**2b** are likely related to the poor π - π overlap in the solid state. In contrast, **3b** was found to behave as an insulator in the thin films in agreement with lack of π - π overlap between the polycyclic backbones in the solid state.

Conclusion

As demonstrated in the above studies, the Scholl reaction of 1,2,4,5-tetra(naphth-2-yl)-3,6-diphenylbenzene can be controlled by properly positioned strong electron-donating groups, leading to two novel types of twisted polycyclic arenes with constitutionally isomeric π -backbones. The polycyclic backbone of **2a,b** is a multiple helicene containing two [5]helicene and four [4]helicene moieties, leading to 24 stereoisomers in principle. Two stereoisomers of **2b**, namely, twisted-**2b** and *anti*-**2b**, were isolated and fully characterized. As monitored with ¹H NMR spectroscopy, the thermal isomerization of twisted-**2b** to the more stable isomer, *anti*-**2b**, is accompanied with an activation free energy of 116 kJ/mol, which is in agreement with the calculated value. **3a,b** are new members of twistacenes with an end-to-end twist of their benzannulated pentacene backbone as found from the crystal structure. Moreover, as found from a brief study on semiconductor properties, twisted-**2b** and *anti*-**2b** functioned as p-type semiconductors in solution-processed thin film transistors with field effect mobility in the range of 10^{-3} cm² V⁻¹ s⁻¹, while **3b** behaved as an insulator in agreement with the lack of π - π overlap between the twisted backbones in the solid state.

Acknowledgements

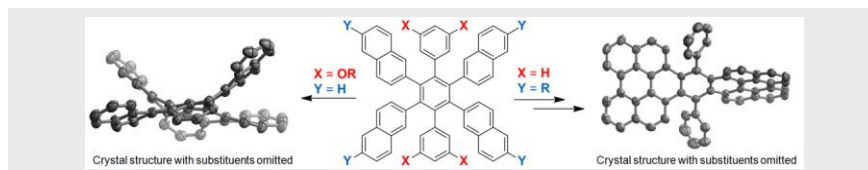
We thank Ms. Hoi Shan Chan (the Chinese University of Hong Kong) for the single crystal crystallography. This work was supported by the Research Grants Council of Hong Kong (CRF C4030-14G) and the Chinese University of Hong Kong (the Faculty Strategic Development Scheme from the Faculty of Science and the One-Off Funding for Research from Research Committee).

Keywords: arenes • polycycles • regioselectivity • oxidative cyclodehydrogenation • organic semiconductors

- [1] M. Grzybowski, K. Skonieczny, H. Butenschön, D. T. Gryko, *Angew. Chem. Int. Ed.* **2013**, *52*, 9900–9930.
- [2] R. Scholl, J. Mansfeld, *Ber. Dtsch. Chem. Ges.* **1910**, *43*, 1734–1746.
- [3] R. Scholl, C. Seer, R. Weitzenböck, *Ber. Dtsch. Chem. Ges.* **1910**, *43*, 2202–2209.
- [4] a) A. Stabel, P. Herwig, K. Müllen, J. P. Rabe, *Angew. Chem.* **1995**, *107*, 1768–1770; *Angew. Chem., Int. Ed.* **1995**, *34*, 1609–1611; b) M. Müller, C. Kübel, K. Müllen, *Chem. Eur. J.* **1998**, *4*, 2099–2109.
- [5] J. Wu, W. Pisula, K. Müllen, *Chem. Rev.* **2007**, *107*, 718–747.
- [6] a) L. Zhi, K. Müllen, *J. Mater. Chem.* **2008**, *18*, 1472–1484; b) A. Narita, X.-Y. Wang, X. Feng, K. Müllen, *Chem. Soc. Rev.* **2015**, *44*, 6616–6643.
- [7] a) K. Kawasumi, Q. Zhang, Y. Segawa, L. T. Scott, K. Itami, *Nat. Chem.* **2013**, *5*, 739–744; b) A. Pradhan, P. Dechambenoit, H. Bock, F. Durolo, *J. Org. Chem.* **2013**, *78*, 2266–2274; c) Y. Sakamoto, T. Suzuki, *J. Am. Chem. Soc.* **2013**, *135*, 14074–14077.
- [8] J. Luo, X. Xu, R. Mao, Q. Miao, *J. Am. Chem. Soc.* **2012**, *134*, 13796–13803.
- [9] K. Y. Cheung, X. Xu, Q. Miao, *J. Am. Chem. Soc.* **2015**, *137*, 3910–3914.
- [10] D. Lungerich, D. Reger, H. Hölzel, R. Riedel, M. M. J. C. Martin, F. Hampel, N. Jux, *Angew. Chem. Int. Ed.* **2016**, *55*, 5602–5605.
- [11] a) C. L. Eversloh, Z. Liu, B. Müller, M. Stangl, C. Li, K. Müllen, *Org. Lett.* **2011**, *13*, 5528–5531; b) S. Xiao, S. J. Kang, Y. Wu, S. Ahn, J. B. Kim, Y.-L. Loo, T. Siegrist, M. L. Steigerwald, H. Li, C. Nuckolls, *Chem. Sci.* **2013**, *4*, 2018–2023; c) H. Kashihara, T. Asada, K. Kamikawa, *Chem. Eur. J.* **2015**, *21*, 6523–6527; d) T. Fujikawa, Y. Segawa, K. Itami, *J. Am. Chem. Soc.* **2015**, *137*, 7763–7768; (e) D. Meng, H. Fu, C. Xiao, X. Meng, T. Winands, W. Ma, W. Wei, B. Fan, L. Huo, N. L. Doltsinis, Y. Li, Y. Sun, Z. Wang, *J. Am. Chem. Soc.* **2016**, *138*, 10184–10190.
- [12] T. Fujikawa, Y. Segawa, K. Itami, *J. Am. Chem. Soc.* **2016**, *138*, 3587–3595.
- [13] R. A. Pascal Jr., *Chem. Rev.* **2006**, *106*, 4809–4819.
- [14] X. Qiao, D. M. Ho, R. A. Pascal Jr., *Angew. Chem., Int. Ed. Engl.* **1997**, *36*, 1531–1532.
- [15] J. Lu, D. M. Ho, N. J. Vogelaar, C. M. Kraml, R. A. Pascal Jr., *J. Am. Chem. Soc.* **2004**, *126*, 11168–11169.
- [16] a) H. M. Duong, M. Bendiko, D. Steiger, Q. Zhang, G. Sonmez, J. Yamada, F. Wudl, *Org. Lett.* **2003**, *5*, 4433–4436; b) J. Xiao, Y. Divayana, Q. Zhang, H. M. Doung, H. Zhang, F. Boey, X. W. Sun, F. Wudl, *J. Mater. Chem.* **2010**, *20*, 8167–8170.
- [17] a) J. Xiao, H. M. Duong, Y. Liu, W. Shi, L. Ji, G. Li, S. Li, X. Liu, J. Ma, F. Wudl, Q. Zhang, *Angew. Chem. Int. Ed.* **2012**, *51*, 6094–6098; b) J. Li, Y. Zhao, J. Lu, G. Li, J. Zhang, Y. Zhao, X. Sun, Q. Zhang, *J. Org. Chem.* **2015**, *80*, 109–113.
- [18] L. Y. Zhai, R. Shukla, R. Rathore, *Org. Lett.* **2009**, *11*, 3474–3477.
- [19] After purification by column chromatography on silica gel once, crude **2a** and **2b** were obtained in a yield of 20% and 33%, respectively, together with unidentified impurities.
- [20] V. J. Chebny, R. Shukla, R. Rathore *J. Phys. Chem. A* **2006**, *110*, 13003–13006.
- [21] L. Zhai, R. Shukla, S. H. Wadumethrige, R. Rathore, *J. Org. Chem.* **2010**, *75*, 4748–4760.
- [22] B. T. King, J. Kroulik, C. R. Robertson, P. Rempala, C. L. Hilton, J. D. Korinek, L. M. Gortari, *J. Org. Chem.* **2007**, *72*, 2279–2288.
- [23] S. Grimme, S. D. Peyerimhoff, *Chem. Phys.* **1996**, *204*, 411–417.
- [24] J. V. Chocholoušová, J. Vacek, A. Andronova, J. Mišek, O. Songis, M. Šámal, I. G. Stará, M. Meyer, M. Bourdillon, L. Pospíšil, I. Stary, *Chem. Eur. J.*, **2014**, *20*, 877–893.
- [25] CCDC 1500317, 1500318 and 1500319 contain the supplementary crystallographic data for twisted-**2a**, *anti*-**2b** and **3b**, respectively. These data can be obtained free of charge from the Cambridge Crystallographic Data Centre via www.ccdc.cam.ac.uk/data_request/cif.
- [26] Y. Shen, C. Chen, *Chem. Rev.* **2012**, *112*, 1463–1535.
- [27] The commonly used formal potential of the redox couple of ferrocenium/ferrocene (Fc⁺/Fc) in the Fermi scale is –5.1 eV, which is calculated on the basis of an approximation neglecting solvent effects using a work function of 4.46 eV for the normal hydrogen electrode (NHE) and an electrochemical potential of 0.64 V for (Fc⁺/Fc) versus NHE. See: C. M. Cardona, W. Li, A. E. Kaifer, D. Stockdale, G. C. Bazan, *Adv. Mater.* **2011**, *23*, 2367–2371.
- [28] E. V. Anslyn and D. A. Dougherty, *Modern Physical Organic Chemistry*, University Science Books: Sausalito, CA, 2004; Chapter 7.
- [29] D. Liu, Z. He, Y. Su, Y. Diao, S. C. B. Mannsfeld, Z. Bao, J. Xu, Q. Miao, *Adv. Mater.* **2014**, *26*, 7190–7196.
- [30] X. Xu, Y. Yao, B. Shan, X. Gu, D. Liu, J. Liu, J. Xu, N. Zhao, W. Hu, Q. Miao, *Adv. Mater.* **2016**, *28*, 5276–5283.
- [31] S. Yang, B. Shan, X. Xu, Q. Miao, *Chem. Eur. J.*, **2016**, *22*, 6637–6642.

Entry for the Table of Contents

COMMUNICATION



Yong Yang, Luyan Yuan, Bowen Shan,
Zhifeng Liu, Qian Miao*

Page No. – Page No.

**Twisted Polycyclic Arenes from
Diphenyltetranaphthylbenzenes by
Controlling the Scholl Reaction with
Substituents**

Two novel types of twisted polycyclic arenes (**2a,b** and **3a,b**) with constitutionally isomeric π -backbones are synthesized by controlling the Scholl reaction of 1,2,4,5-tetra-naphthyl-3,6-diphenylbenzene with properly positioned electron-donating substituents.